

Atomic Force Microscopy of Plant-Parasitic Nematodes

A. CIANCIO¹

Abstract: A simple method for atomic force microscopy (AFM) of nematode cuticle was developed to visualize the external topography of *Helicotylenchus lobus*, *Meloidogyne javanica*, *M. incognita*, and *Xiphinema diversicaudatum*. Endospores of two isolates of the nematode parasite, *Pasteuria penetrans*, adhering to *M. incognita* and *X. diversicaudatum* were also visualized and measured by this technique. Scanning procedures were applied to specimens killed and dehydrated in air or dehydrated and stored in glycerol. Atomic force microscopy scanning of nematodes in constant height mode yielded replicated high-resolution images of the cuticle showing anatomical details such as annulations and lateral fields. Submicrometer scale images allowed the identification of planar regions for further higher resolution scans.

Key words: atomic force microscope, AFM, cuticle, endospore, morphology, nematode, *Pasteuria penetrans*, scanning probe microscopy, ultrastructure.

Atomic force microscopy (AFM) and scanning tunneling microscopy (STM) are techniques of recent introduction that provide high resolution and atomic scale images of a number of substrates, including some biological molecules (1,2,6,7). Both techniques are based on the exploitation of the low-scale interactions occurring between the substrate and an extremely (a few atoms) fine apex tip placed at a distance of a few nanometers from the substrate.

Scanning tunneling microscopy exploits tunneling currents that occur between the substrate and atoms on the tip. In AFM, the tip is held by a thin cantilever and a laser beam is pointed on its upper side. The topographic data on the sample are obtained measuring the deflections induced by the substrate on the cantilever by means of two photodetectors reading the intensity of the reflected laser light. The analogic information obtained at each step of the scanning procedure is then used in both techniques to reconstruct the original sample topography. Signals are converted to numerical data through a digital signal processor, and appropriate software is used for graphic display. The sample images are formed through an X, Y, Z scan-

ning procedure achieved through piezoelectric components that move the tip or the sample (6,7).

Molecular resolution images of DNA, proteins, and other biomolecules have been obtained through STM, as well as atomic resolution images of graphite and other inorganic and organic conductive materials (5-7,10). Similarly, AFM has provided images of DNA and other non-conductive biomolecules for which STM cannot be applied (4,8,9,13). Biomolecules and a number of biological surfaces can be visualized by AFM even without any previous sample preparation, allowing the scanning of living cells or tissues in water and other fluids (3,7,9).

The potential of AFM for yielding information on nematode morphology, cuticular topography, ultrastructure, and composition should be explored. Initial results from a number of experiments carried out with plant-parasitic nematodes and comparison of AFM with scanning electron microscopy (SEM) technique are presented herein.

MATERIALS AND METHODS

Nematode species and preparation: The species used were *Xiphinema diversicaudatum* (Micoletzky) Thorne, originating from a population found parasitizing peach at Borgo d'Ale, Italy, and associated with a specific *Pasteuria penetrans* (ex Thorne) Sayre & Starr isolate; *Helicotylenchus lobus* Sher, from a population found at River-

Received for publication 11 April 1994.

¹ Istituto di Nematologia Agraria, C.N.R., Via Amendola 165/A, 70126 Bari, Italy.

The author acknowledges Professor R. Mankau and Dr. M. Mundo-Ocampo, University of California, Riverside, for providing some of the biological samples examined and assistance with scanning electron microscopy, respectively.

side, California, from turfgrass; *Meloidogyne incognita* (Kofoid & White) Chitwood, from a population in greenhouse soil at Riverside and artificially infected with *P. penetrans*; and *M. javanica* (Treub) Chitwood, from a population from Acireale, Italy, maintained on tomato. The specimens examined were extracted from soil with Cobb's sieving and decanting technique, fixed in 2.5% formalin, and dehydrated to glycerol with a slow method (12).

Adult and juvenile *X. diversicaudatum* and juveniles of *M. javanica* were placed in a droplet of sterile distilled water on a glass slide, killed with gentle heat, and transferred to a droplet of ultrapure distilled water in the center of a 10-mm-d steel stub. Specimens of *X. diversicaudatum* were cut into three or four parts with a sharp cutting blade or fractured edge of a glass pipette tip, directly on the stub. Subsequently, the nematodes were air-dried for a few minutes on a mild heat source (35–40 C) and scanned.

Second-stage *M. incognita* juveniles fixed in 2.5% formalin from a long-term fixed collection and stored at room temperature in glass vials were scanned. The juveniles were picked up from the suspension and examined at $\times 312$ with a light microscope to determine the presence of *P. penetrans* endospores adhering to the cuticle. Specimens with endospores were washed in a water droplet and air-dried at room temperature.

Glycerol-dehydrated *H. lobus* from a long-term collection and juveniles of *X. diversicaudatum* with adhering *P. penetrans* endospores were scanned after two washings in 95% ethanol droplets for a few seconds. The images obtained from *H. lobus* were compared with SEM images taken in the same regions from other glycerol-dehydrated specimens. For SEM of *H. lobus*, specimens were fixed in 5% formalin, dehydrated, and slowly infiltrated with glycerol, coated with 20-nm gold palladium, and examined with a Jeol 35-C at 5 kV.

Scanning: Samples were placed on a type-D head scanner of an AFM Nano-

scope II (Digital Instruments, Santa Barbara, CA). Silicon nitride triangular cantilevers with wide legs (200- μm length; spring constant 0.12 N/m, Digital Instruments) were used for nematode scanning in air at room temperature and pressure. Different scan sizes (1–14 μm) and scan speeds with 400 sample points per line were used at zero set-point voltage. Images were captured in constant height mode, with sample vertical displacements set to maintain a constant difference of the photodetector readings. A number of different tips and series of scanings were used to obtain a sufficient amount of replications. The images usually were not digitally filtered. The sample was manually positioned below the tip by moving the shim through the scanning head aperture with a pair of tweezer tips, then adjusting the tip orientation with the microscope adjustment screws. To increase the probability of scanning a large portion of the cuticle, the tip was usually placed at the center of the samples, then lowered until it was directly in contact with the sample (as revealed by the changes in the readings on the laser light detector) and subsequently raised a few micrometers. Alternatively, the tip was lowered close to the sample without touching it. Measurements were performed with the device software utilities directly on the graphic display. The head was calibrated with a gold calibration ruler with 1- μm -wide serial incisures. Images were photographed from the screen with a 70–200 zoom at 0.5–1 second exposure times.

RESULTS

Scanning nematodes in constant height mode yielded replicated images of the cuticle topography for all the species tested (Figs. 1–3). Adhesive forces occurring between the metal stub and the nematode cuticle after drying were usually sufficient to avoid sample displacement during scanning. For large scans, the scan rates applied varied between 5.76 and 19.53 Hz with linear input data. Each image had an optimal scan speed for image quality and

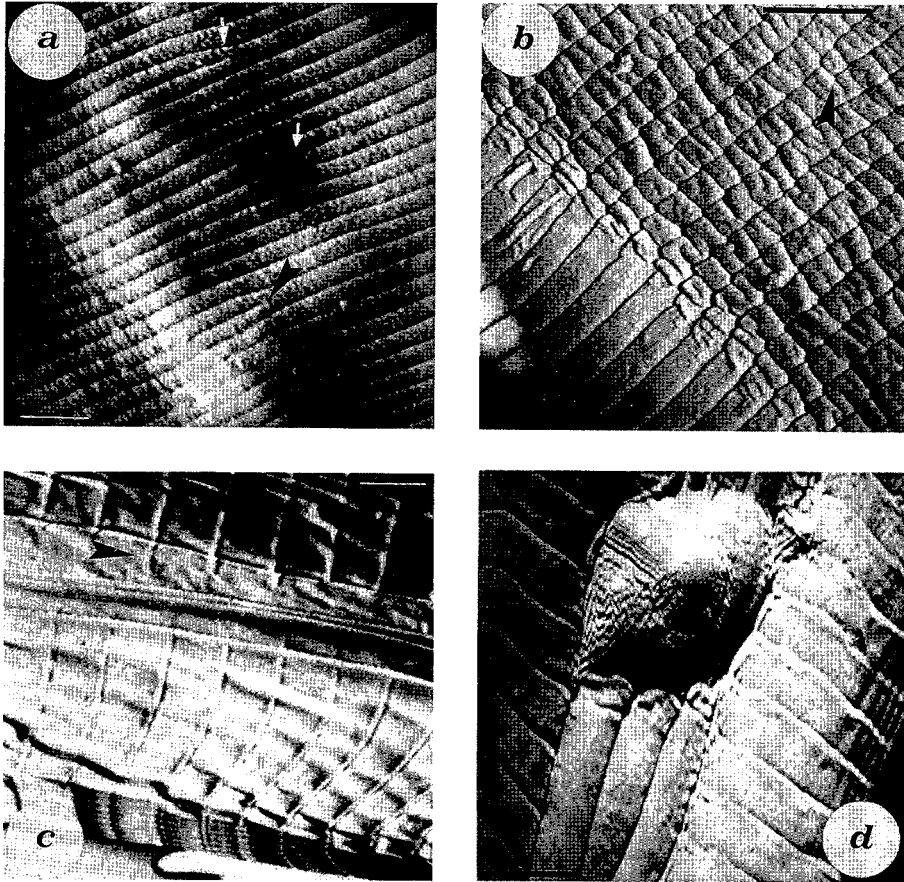


FIG. 1. Top view atomic force microscopy images of the cuticle surface of nematodes. A) Annulations and anastomoses (arrows) from air-dried cuticle of a *Xiphinema diversicaudatum* female. B) Air-drying-induced distortion of the cuticle of a *X. diversicaudatum* male. C) Lateral fields and insertions (arrows) of cuticular annulations from air-dried juvenile *Meloidogyne javanica*. D) Endospore of *Pasteuria penetrans* adhering to a juvenile *Meloidogyne incognita*. Scale bars: a = 2.2 μm ; b = 1.4 μm ; c = 2.0 μm ; d = 2.2 μm .

resolution. Vertical scales used to obtain the image data ranged from 0.3 to 4.5 nanoamps. Integral and proportional gain

settings ranged from 3.0 to 3.6 and 2.6 to 5.1, respectively.

Several replicated scans without cuticu-

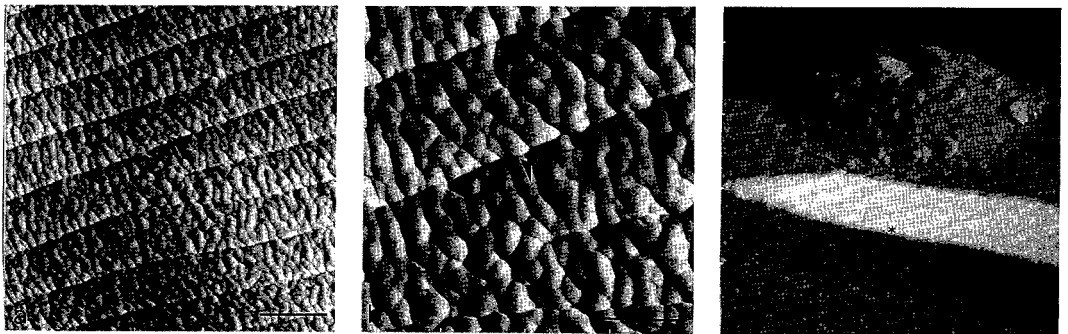


FIG. 2. A,B) Atomic force microscopy scanning of cuticular fiber-like elements from an air-dried *Xiphinema diversicaudatum* female at different magnifications. Arrow heads point to the same sample region. C) Endospore of *Pasteuria penetrans* on a glycerol-dehydrated juvenile *X. diversicaudatum*. Asterisk indicates an area of loss in signal detection due to a cuticle deformation (c). Scale bars: a = 1.0 μm ; b = 0.5 μm ; c = 2.0 μm .

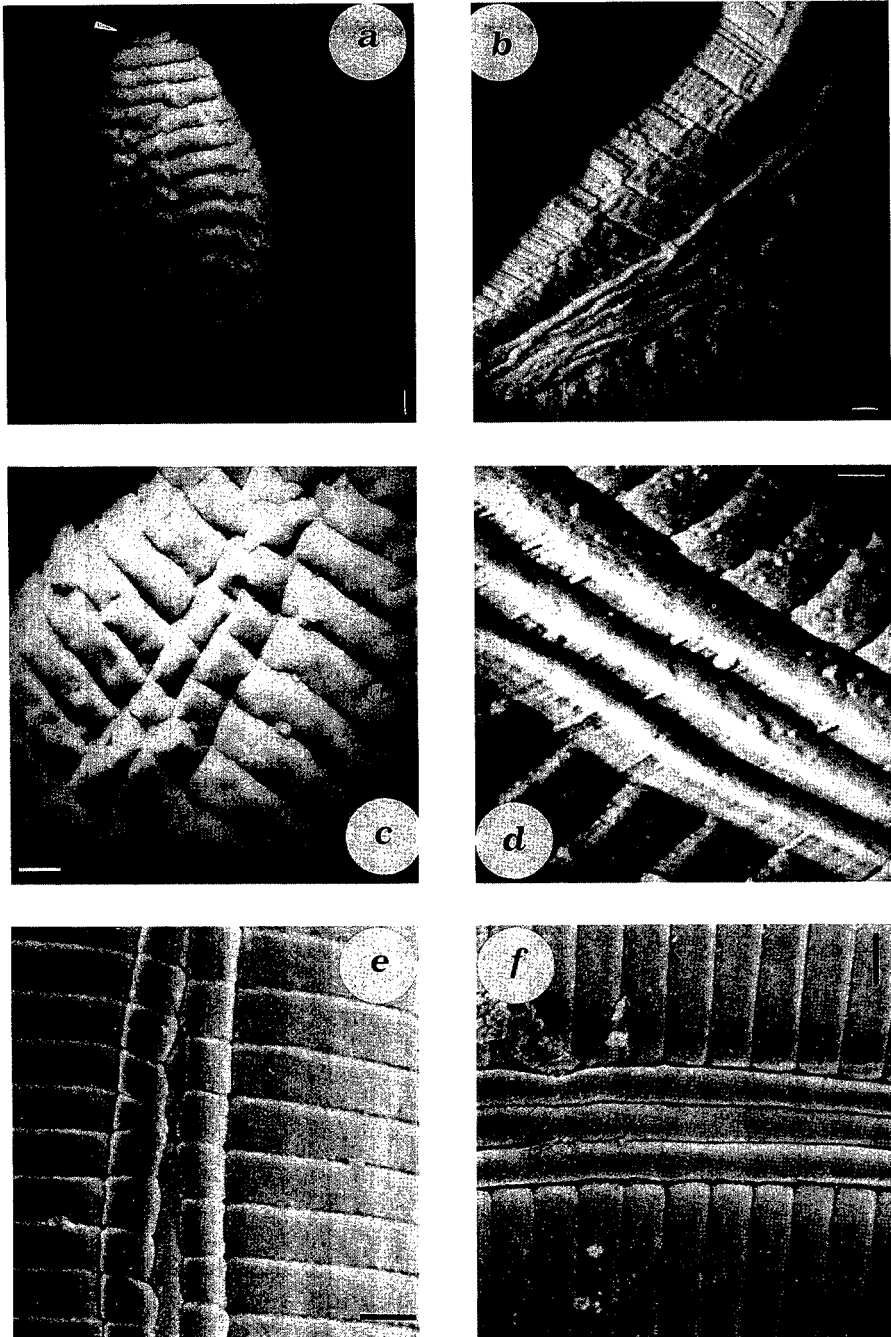


FIG. 3. Atomic force microscopy (AFM) and scanning electron microscopy (SEM) images of glycerol-dehydrated specimens of *Helicotylenchus lobus*. A–D) AFM images. A) Head region showing lips (arrow). B) Caudal region. C) Lateral field cephalic region. D) Lateral field, midbody. E,F) SEM images. E) Lateral field, cephalic region. F) Lateral field, midbody. Scale bars: a,b = 0.75 μm ; c = 2.0 μm ; d = 1.0 μm ; e,f = 2.0 μm .

lar damage were usually obtained at the zero setpoint scan voltage setting with an initial photodetector difference between -2 and -6 volts. Dried cuticle usually

supported the pressure of contact between sample and tip. In a few cases, abrasions and marks were produced with photodetector differences of -10 volts. Tip mi-

cropositioning and orientation over the sample were also performed during scanning by adjusting screws for image centering. This procedure, however, resulted in a higher rate of tip distortion and crashing.

In a 14.0- μm scan of *X. diversicaudatum*, details of the cuticular annulations were observed (Fig. 1A,B). Annule width was 0.4–0.5 μm , with anastomoses appearing frequently at 2–7 annulation intervals (1.4–3.6 μm). An unfixed, dead female specimen coated with a felt of bacterial microflora (*Clostridium* sp.) developing on the cuticle showed, after bacteria were gently removed, a different cuticular organization with apparent fiber-like elements. These elements were 100–200 nm wide with regular crossings at 45–50° of the longitudinal body direction and were present over the entire nematode body. They had a regular shape and dimensions different from the dehydration-induced folds observed on other fixed specimens (Fig. 1B). Several replicated scans were obtained from this specimen at different resolutions and scan angles (Fig. 2A,B). In all cases the fiber-like pattern retained the cuticular organization, with annulations visible at 0.5–0.6 μm intervals.

Annulations 1.1–1.4 μm wide were observed in a 10- μm -scan of *M. javanica* juveniles (Fig. 1C). The images showed lateral fields 1.7–2.1 μm wide and partial areolation of the lateral field incisures.

Infective endospores of *P. penetrans* were visualized on *M. incognita* juveniles and on specimens of *X. diversicaudatum*. Diameter of endospores on *M. incognita* measured 3.5–4.2 μm , whereas those on *X. diversicaudatum* measured 6.5–7.2 μm (Figs. 1D,2C). The images showed some details of endospore organization (e.g., the central core area and the matrix of the parasporal fibers). Endospores of the isolate from *X. diversicaudatum* had a concavity on the endospore apex (Fig. 2C), probably an artifact.

Glycerol-dehydrated *H. lobus* allowed the scanning of both the head and tail regions, together with mid-body areas. The

images showed transverse, 1.8- μm -wide annules; the lateral fields (Fig. 3D); the oral disc; the beginning of lateral incisures in the cephalic region (Fig. 3A,C); and additional incisures visible at the end of the lateral field, in the tail region (Fig. 3B). Although AFM showed nematode details similar to those obtained with SEM for the same species in the same regions, the image quality and resolution at the same magnification levels appeared superior in SEM images (Fig. 3E–F).

No differences in image quality were observed between air-dried or glycerol-dehydrated specimens, although air-drying produced a higher number of sample distortions. Glycerol-embedded nematodes washed and dried on the stub showed mild flattenings and distortions. Sample distortions (Fig. 1B), body curvature (Fig. 1C), areas of failed tip engagement (Fig. 3A–C), or failed signal detection (Fig. 2C) were responsible for some image shadowing.

DISCUSSION

Present results of scanning flat areas of nematode cuticle provide a basis useful for future higher magnification scans. The AFM large scans of *X. diversicaudatum* and *M. javanica* showed a number of details difficult to resolve with traditional light microscopy and usually visualized only with SEM. The quality of AFM of the surface appears comparable with that of similar SEM images of the same nematode species or *Pasteuria* isolates (11). Because of probe pyramidal shape and dimensions, AFM offers a reduced vertical field depth with respect to SEM. AFM, however, can yield progressively higher enlargements with little loss of resolution (Fig. 2A,B). This progressive zooming of a sample is difficult to achieve with SEM due to electron wavelength limitations. The AFM cantilever is deflected during scanning by sample-tip contact or repulsive forces and follows the sample surface contour acting as a profilometer. Resolution depends on force settings, piezo and tip sensitivities,

and tip sharpness. It is not influenced by laser wavelength (7).

AFM appears as a technique integrative to actual SEM methods applied to nematodes, with promising possibilities at sub-micrometer scales. The most interesting feature of this technique is the possibility of scanning nematodes without any previous fixation or manipulation. Apart from a higher frequency of distortions associated with the different drying procedures, no other structural differences were observed between the cuticle of nematodes air-dried immediately after killing and that of glycerol-dehydrated samples. The AFM images in both cases were obtained directly from the cuticle surface and, unlike SEM, were not affected by metal coatings or vacuum exposure. A more standard and appropriate procedure for rapid drying (e.g., vacuum freeze or critical point) should further reduce distortions, particularly of small and delicate specimens. Methods for nematode immobilization or anesthesia are required for scanning living specimens.

Measurement scales of images require a previous accurate calibration of the scanning head, especially when data on fine details are required. Although height-mode scanning provides an apparent three-dimensional cuticle representation, the scanning procedure is obtained through step-by-step sample displacement under the tip. At each point the image displays the vertical heights of the sample or the measured forces through different colors or color intensities. Distortions or artifacts are primarily related to vibrations or to sample orientations rather than perspective effects. This property is useful for collecting quantitative data on small anatomical details such as cuticular annulations, or for measurement of *P. penetrans* endospores and their structural components. Additional applications to nematodes and other invertebrates include resolution of small or planar cuticular structures such as

amphids, natural openings or pores, analysis of cuticle organization and layers, and direct imaging of viruses and other cuticle-associated microorganisms.

LITERATURE CITED

1. Binnig, G., H. Rohrer, C. Gerber, and E. Weibel. 1982. Surface studies by scanning tunneling microscopy. *Physical Review Letters* 49:57-61.
2. Binnig, G., C. F. Quate, and C. Gerber. 1986. Atomic force microscopy. *Physical Review Letters* 56: 930-933.
3. Butt, H. J., E. K. Wolff, S. A. C. Gould, B. D. Northern, C. M. Peterson, and P. K. Hansma. 1990. Imaging cells with the atomic force microscope. *Journal of Structural Biology* 105:54-61.
4. Chernoff, E. A. G., and D. A. Chernoff. 1992. Atomic force microscope images of collagen fibers. *Journal of Vacuum Science Technology A* 10:596-599.
5. Driscoll, R. J., M. G. Youngquist, and J. D. Baldeschwieler, 1990. Atomic scale imaging of DNA using scanning tunneling microscopy. *Nature* 346:294-296.
6. Hansma, P. K., and J. Tersoff. 1987. Scanning tunneling microscopy. *Journal of Applied Physics* 61: 1-23.
7. Hansma, P. K., V. B. Elings, O. Marti, and C. E. Braker. 1988. Scanning tunneling and atomic force microscopy: Application to biology and technology. *Science* 242:209-216.
8. Hansma, H. G., J. Vesenska, C. Siegerist, G. Kelderman, H. Morrett, R. L. Sinsheimer, V. Elings, C. Bustamante, and P. K. Hansma. 1992. Reproducible imaging and dissection of plasmid DNA under liquid with the atomic force microscope. *Science* 256: 1180-1184.
9. Henderson, E., P. G. Haydon, and D. S. Sakaguchi. 1992. Actin filaments dynamics in living glial cells imaged by atomic force microscopy. *Science* 257: 1944-1946.
10. Lindsay, S. M., T. Thundat, L. Nagahara, U. Knipping, and R. L. Rill. 1989. Images of DNA double helix in water. *Science* 244:1063-1064.
11. Sayre, R. M., and W. P. Wergin. Bacterial parasite of a plant nematode: Morphology and ultrastructure. *Journal of Bacteriology* 129:1091-1101.
12. Southey, J. F. 1970. *Laboratory methods for work with plants and soil nematodes*. Technical Bulletin No. 2. London: Her Majesty's Stationery Office.
13. Weisenhorn, A. L., M. Egger, F. Ohnesorge, S. A. C. Gould, S. P. Heyn, H. G. Hansma, R. L. Sinsheimer, H. E. Gaub, and P. K. Hansma. 1991. Molecular resolution images of Langmuir-Blodgett films and DNA by atomic force microscopy. *Langmuir* 7: 8-12.